Mn_2O_3 Nanoparticles Synthesized from Thermal Decomposition of Manganese(II) Schiff Base Complexes

A.D. Khalaji[a,*] and M. Ghorbani[b]

[a]Department of Chemistry, Faculty of Science, Golestan University, Gorgan, Iran

[b]Department of Chemistry, Payame Noor University, P.O. Box 19395-3697, Tehran, Iran

(Received May 14, 2017; in final form October 4, 2017)

The Mn_2O_3 nanoparticles have been prepared using solid state thermal decomposition of Mn$\mathbf{L}^1$ and Mn$\mathbf{L}^2$, $\mathbf{L}^1$ = *N*,*N*′-bis(2-hydroxy-4-methoxybenzophenone)-1,3-propanediamine and $\mathbf{L}^2$ = *N*,*N*′-bis(2-hydroxy-4-methoxybenzophenone)-1,2-cyclohexanediamine, at 500 °C for 3 h and characterized by the Fourier transform infrared spectroscopy, X-ray powder diffraction and scanning electron microscopy. The Fourier transform infrared spectroscopy and X-ray powder diffraction confirm that the formed product at 500 °C is Mn_2O_3. The Mn$\mathbf{L}^1$ and Mn$\mathbf{L}^2$ complexes were prepared from the one-pot reaction of $MnCl_2{\cdot}H_2O$, diamine and 2-hydroxy-4-methoxybenzophenone and characterized by elemental analyses, the Fourier transform infrared spectroscopy and thermogravimetry.

DOI: 10.12693/APhysPolA.133.7

PACS/topics: Mn_2O_3 nanoparticles, manganese(II), Schiff base, thermal decomposition

1. Introduction

Recently, transition metal oxide nanostructures such as CuO [1, 2], Co_3O_4 [3, 4], NiO [5], ZnO [6] and Cr_2O_3 [7] have been actively studied by many groups due to various properties and applications [1–7]. Among the transition metals, manganese exhibits several oxidation state and forms different oxides such as MnO [8, 9], Mn_2O_3 [10, 11], Mn_3O_4 [8–11], and MnO_2 [8]. Manganese oxides are an important class of transition metal oxide family due to unique chemical and physical properties [8–11]. Among the different oxidation state of manganese oxides, Mn_2O_3 nanoparticles are well-known as non-toxic, cheap, environmentally friendly and abundant and widely investigated as anode materials for lithium ion batteries because of their large theoretical specific capacities [12–14], catalyst [15, 16] and hydrazine electrochemical sensing [17]. Recently, Mn_2O_3 has been prepared by thermal decomposition of different manganese precursors [12, 13, 17, 18], hydrothermal [14], solvothermal [16] and wet chemical approach [15]. Among the various methods available for synthesis of transition metal oxides nanoparticles, thermal decomposition is a simple, cost effective and eco-friendly [19–21]. Thermal decomposition is chemical decomposition caused by heat. Several experimental efforts have been carried out for synthesis of Mn_2O_3 nanoparticles by thermal decomposition of various precursors such as $MnCO_3$ [13, 18] and $Mn(OH)_2$ [12].

In this work, Mn_2O_3 nanoparticles were synthesized from the Schiff base complexes Mn$\mathbf{L}^1$ and Mn$\mathbf{L}^2$ (Fig. 1) as new precursors by solid state thermal decomposition at 500 °C for 3 h.

*corresponding author; e-mail: alidkhalaji@yahoo.com

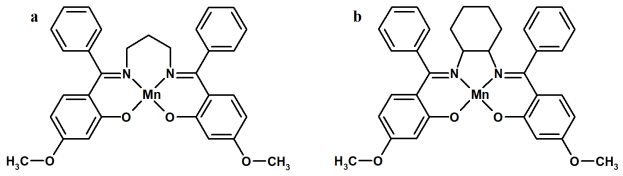

Fig. 1. Chemical structure of (a) Mn$\mathbf{L}^1$ and (b) Mn$\mathbf{L}^2$.

2. Experimental

2.1. Material and method

All reagents and solvents for synthesis and analysis were commercially available and used as received without further purifications. Elemental analyses were carried out using a Heraeus CHN–O–Rapid analyzer, and results agreed with calculated values. The Fourier transform infrared (FT-IR) spectra were recorded as a KBr disk on a FT-IR Perkin–Elmer spectrophotometer. The thermogravimetric/differential thermal analysis (TG/DTA) were performed on a Perkin Elmer TG/DTA lab system 1 (Technology by SII) in nitrogen atmosphere with a heating rate of 20 °C/min in the temperature span of 50–800 °C. X-ray powder diffraction (XRD) pattern of the complex was recorded on a Bruker AXS diffractometer D8 ADVANCE with Cu K_α radiation with nickel beta filter in the range $2\theta = 10°-80°$. The scanning electron microscopy (SEM) images were obtained from a Philips XL-30ESEM.

2.2. Preparation of *Mn*$\mathbf{L}^1$ and *Mn*$\mathbf{L}^2$

A solution of 1,3-butanediamine or 1,2-cyclohexanediamine (1 mmol) in 15 mL ethanol is added drop-wise to an ethanol solution of 2-hydroxy-4-methoxybenzophenone (0.046 g, 2 mmol) under stirring condition. The reaction mixture is then refluxed for

2 h when the solution color turns yellow. Then, a solution of $MnCl_2{\cdot}6H_2O$ (1 mmol in 15 mL ethanol) was added drop-wise. After the addition was completed, the stirring was continued for 2 h. The brown precipitates of complexes were filtered and washed with cold ethanol and dried at room temperature.

Analytical calculation. for $C_{31}H_{28}N_2MnO_4$ (Mn$\mathbf{L}^1$): C, 68.00.; H, 5.12.; N, 5.12%. Found; C, 68.05.; H, 5.09.; N, 5.18%. FT-IR (KBr, cm^{-1}): 2873-3050 (C-H aromatic and aliphatic), 2806 (–CH=N), 1567 (–C=N–).

Analytical calculation. for $C_{34}H_{30}N_2MnO_4$ (Mn$\mathbf{L}^2$): C, 69.74.; H, 5.13.; N, 4.77%. Found; C, 69.81.; H, 5.16.; N, 4.65%. FT-IR (KBr, cm^{-1}): 2873-3059 (C-H aromatic and aliphatic), 2807 (–CH=N), 1573 (–C=N–).

2.3. Preparation of Mn_2O_3 nanoparticles

The Schiff base complexes were loaded into a platinum crucible and placed in oven and heated at a rate of 10 °C min^{-1} in air. Nanoparticles of Mn_2O_3 were obtained at 500 °C after 3 h. The final products were washed with ethanol to remove impurities, if any, and dried at room temperature for several days. The synthesized Mn_2O_3 nanoparticles were characterized by FT-IR, XRD, and SEM.

3. Results and discussion

3.1. Schiff base complexes

The one-pot reaction in ethanol of 1:2:1 molar mixture of diamine, 2-hydroxy-4-methoxybenzophenone and $MnCl_2{\cdot}6H_2O$ produced the Schiff base complexes Mn$\mathbf{L}^1$ and Mn$\mathbf{L}^2$. The elemental analyses are in good agreement with formula proposed for complexes.

In the FT-IR spectra of Mn$\mathbf{L}^1$ and Mn$\mathbf{L}^2$, the absence of vibration peak related to OH, NH_2 and C=O groups and appearance of new peaks at 1567 cm^{-1} for Mn$\mathbf{L}^1$ and 1572 cm^{-1} for Mn$\mathbf{L}^2$ have suggested formation of the Schiff base ligands, and coordinated to manganese ions as dianionic form coordinate as tetradentate. Also, the FT-IR bands at about 3000 and 2810 cm^{-1} have been assigned to C–H and –CH=N– groups. In the range of 1450–1550 cm^{-1}, the bands characteristic for vibration mode of C=C of the aromatic rings can be observed [22, 23]. The bands located in about 1180 cm^{-1} are assigned to C–O vibration [22, 23]. Additional two bands at 409 cm^{-1} and 515 cm^{-1} assigned to stretching vibrations M–N and M–O can be observed in the spectra of complexes [22, 23].

The TG curves of Mn$\mathbf{L}^1$ and Mn$\mathbf{L}^2$ under argon atmosphere are given in Fig. 2. The decomposition patterns of Mn$\mathbf{L}^1$ and Mn$\mathbf{L}^2$ are quite similar. The complexes are stable up to ≈ 200 °C and during further heating undergo decomposition in two stages. In the first stage, the complexes Mn$\mathbf{L}^1$ and Mn$\mathbf{L}^2$ show a mass loss of 25% and 40%, respectively, in the temperature range 200–370 °C. In the second stage, from 370 to 520 °C, the complexes Mn$\mathbf{L}^1$ and Mn$\mathbf{L}^2$ show mass loss of 50% and 40%, respectively.

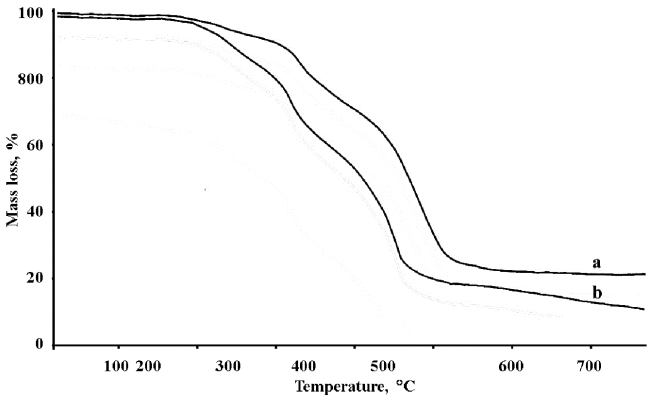

Fig. 2. TG curves of Mn$\mathbf{L}^1$ and Mn$\mathbf{L}^2$.

3.2. Mn_2O_3 nanoparticles

For preparation of Mn_2O_3 nanoparticles, the Schiff base complexes were calcinated at 500 °C for 3 h. The FT-IR spectra of the Mn_2O_3 nanoparticles are shown in Fig. 3. The peaks at about 3390 and 1605 cm^{-1} can be assigned to O–H stretching and binding vibration of H_2O molecules adsorbed on the surface of Mn_2O_3 nanoparticles, respectively [22]. The two peaks appearing at 576 and 475 cm^{-1} are assigned to the Mn–O–Mn asymmetric stretching and bending vibration mode, respectively [22]. Comparison of the FT-IR spectra of complexes and nanoparticles (Fig. 3) suggests that the manganese complexes transform to Mn_2O_3 at 500 °C.

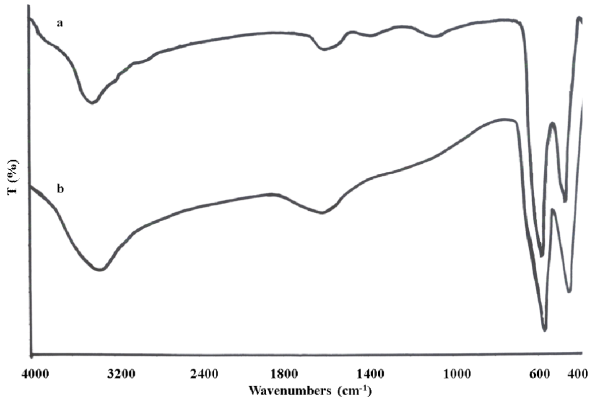

Fig. 3. FT-IR spectra of Mn_2O_3 nanoparticles prepared from (a) Mn$\mathbf{L}^1$ and (b) Mn$\mathbf{L}^2$.

Figure 4 shows the XRD patterns of Mn_2O_3 nanoparticles. Pure cubic structure of Mn_2O_3 nanoparticles with lattice parameters of $a = b = c = 0.9411$ nm (JCPDS card No. 24-0508) are obtained [13] without other impurities. According to the Scherrer formula, the as-obtained Mn_2O_3 nanoparticles have an average size of 27.59 nm for nanoparticles prepared from Mn((MeO–bph)$_2$pn) and 24.47 nm for nanoparticles prepared from Mn((MeO–bph)$_2$hn) corresponds to the (222) plane of the cubic Mn_2O_3 nanoparticles.

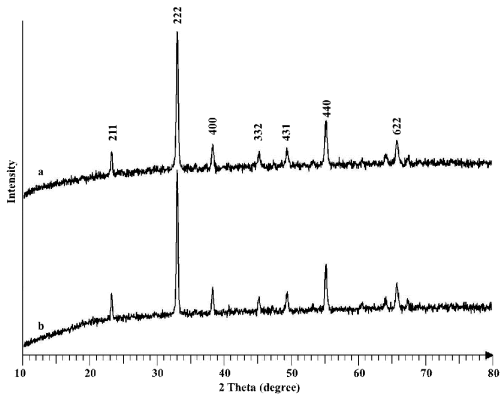

Fig. 4. XRD pattern of Mn_2O_3 nanoparticles prepared from (a) Mn$\mathbf{L}^1$ and (b) Mn$\mathbf{L}^2$.

The morphology of the obtained Mn_2O_3 nanoparticles was further investigated by SEM. Figure 5 shows the SEM images of the obtained Mn_2O_3 nanoparticles from the Schiff base complexes Mn$\mathbf{L}^1$ and Mn$\mathbf{L}^2$ at 500 °C. It can be observed that with change the precursor from Mn$\mathbf{L}^1$ to Mn$\mathbf{L}^1$, the size, morphology and agglomeration of the obtained Mn_2O_3 nanoparticles were changed.

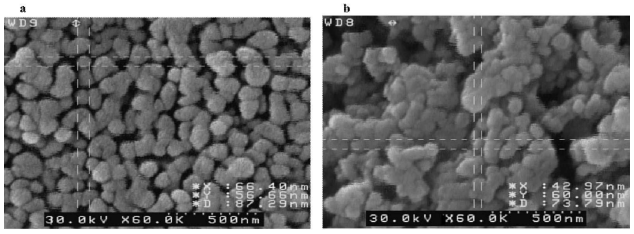

Fig. 5. SEM images of Mn_2O_3 nanoparticles prepared from (a) Mn$\mathbf{L}^1$ and (b) Mn$\mathbf{L}^2$.

Conclusions

Mn_2O_3 nanoparticles have been prepared by a solid-state thermal decomposition of Mn(II) Schiff base complexes at 500 °C. The crystallite size and shape of Mn_2O_3 nanoparticles are quite different from each other. This method is facile, nontoxic and inexpensive.

Acknowledgments

The financial support from the Golestan University is gratefully acknowledged.

References

[1] D. Chi, H. Yang, Y. Du, T. Lv, G. Sui, H. Wang, J. Lu, *RSC Adv.* **4**, 37329 (2014).

[2] P.K. Raul, S. Senapati, A.K. Sahoo, L.M. Umlong, R.R. Devi, A.J. Thakur, V. Veer, *RSC Adv.* **4**, 40580 (2014).

[3] S.A. Makhlouf, Z.H. Bakr, K.I. Aly, M.S. Moustafa, *Superlatt. Microstruct.* **64**, 107 (2013).

[4] Y. Lv, Y. Lv, W. Shen, *Catal. Commun.* **42**, 116 (2013).

[5] Y. Zhu, H. Guo, Y. Wu, C. Cao, S. Tao, Z. Wu, *J. Mater. Chem. A* **2**, 7904 (2014).

[6] Y. Pushpanathan, D. Suresh Kumar, *J. Nanostruct. Chem.* **4**, 95 (2014).

[7] Z. Pei, X. Zhang, *Mater. Lett.* **93**, 377 (2013).

[8] J. Yue, L. Chen, N. Wang, X. Jiang, H. Xu, J. Yang, Y. Qian, *J. Mater. Chem. A* **2**, 17421 (2014).

[9] I. Rusakova, T. Ould-Ely, C. Hofmann, D. Prieto-Centurion, C.S. Levin, N.J. Halas, A. Luttge, K.H. Whitmire, *Chem. Matter.* **19**, 1369 (2007).

[10] Y.-F. Han, F. Chen, Z. Zhong, K. Ramesh, L. Chen, E. Widjaja, *J. Phys. Chem. B* **110**, 24450 (2006).

[11] Z. Chen, Z. Jiao, D. Pan, Z. Li, M. Wu, C.-H. Shek, C.M. Lawrence Wu, J.K.L. Lai, *Chem. Rev.* **112**, 3833 (2012).

[12] X. Zhang, Y. Qian, Y. Zhu, K. Tang, *Nanoscale* **6**, 1725 (2014).

[13] Y. Deng, Z. Li, Z. Shi, H. Xu, F. Peng, G. Chen, *RSC Adv.* **2**, 4645 (2012).

[14] Y. Dai, H. Jiang, Y. Hu, C. Li, *RSC Adv.* **3**, 19778 (2013).

[15] H. Rahaman, R.M. Laha, D.K. Maiti, S.K. Ghosh, *RSC Adv.* **5**, 33923 (2015).

[16] X. Niu, H. Wei, K. Tang, W. Liu, G. Zhao, Y. Yang, *RSC Adv.* **5**, 66271 (2015).

[17] B. Zhou, J. Yang, X. Jiang, *Mater. Lett.* **159**, 362 (2015).

[18] M. Pudukudy, Z. Yaakob, R. Rajendran, *Mater. Lett.* **136**, 85 (2014).

[19] E. Shahsavani, N. Feizi, A.D. Khalaji, *J. Ultrafine Grain. Nanostruct. Mater.* **49**, 48 (2016).

[20] M. Salavati-Niasari, F. Davar, M. Mazaheri, *Polyhedron* **27**, 3467 (2008).

[21] I. Sharifi, A. Zamanian, A. Behnamghader, *J. Ultrafine Grain. Nanostruct. Mater.* **49**, 87 (2016).

[22] M. Salavati-Niasari, M. Esmaeili-Zare, M. Gholami-Daghian, *Adv. Powder Technol.* **25**, 879 (2014).

[23] I. Alan, A. Kriza, M. Badea, N. Stanica, *J. Therm. Anal. Calorim.* **111**, 483 (2013).